HHS Public Access

Author manuscript

*J Hepatol*. Author manuscript; available in PMC 2022 September 07.

Published in final edited form as:

*J Hepatol*. 2022 September ; 77(3): 619–631. doi:10.1016/j.jhep.2022.04.010.

# Lack of VMP1 impairs hepatic lipoprotein secretion and promotes non-alcoholic steatohepatitis

**Xiaoxiao Jiang**[1], **Sam Fulte**[1], **Fengyan Deng**[1], **Shiyuan Chen**[2], **Yan Xie**[3], **Xiaojuan Chao**[1], **Xi C. He**[2], **Yuxia Zhang**[1], **Tiangang Li**[4], **Feng Li**[5], **Colin McCoin**[6], **E. Matthew Morris**[6], **John Thyfault**[6], **Wanqing Liu**[7], **Linheng Li**[2,8], **Nicholas O. Davidson**[3], **Wen-Xing Ding**[1], **Hong-Min Ni**[1,*]

[1]Department of Pharmacology, Toxicology and Therapeutics, University of Kansas Medical Center, Kansas City, KS, USA

[2]Stowers Institute for Medical Research, Kansas City, MO, USA

[3]Division of Gastroenterology, Department of Medicine, Washington University School of Medicine, St. Louis, MO, USA

[4]Department of Physiology, Harold Hamm Diabetes Center, University of Oklahoma Health Sciences Center, Oklahoma City, OK, USA

[5]Department of Pathology & Immunology, Baylor College of Medicine, Houston, TX, USA

[6]Department of Physiology, University of Kansas Medical Center, Kansas City, KS, USA

[7]Department of Pharmaceutical Sciences, Wayne State University, Detroit, MI, USA

[8]Department of Pathology, University of Kansas Medical Center, Kansas City, KS, USA

## Abstract

**Background & Aims:** Vacuole membrane protein 1 (VMP1) is an endoplasmic reticulum (ER) transmembrane protein that regulates the formation of autophagosomes and lipid droplets. Recent evidence suggests that VMP1 plays a critical role in lipoprotein secretion in zebra fish and cultured cells. However, the pathophysiological roles and mechanisms by which VMP1 regulates lipoprotein secretion and lipid accumulation in non-alcoholic fatty liver disease (NAFLD) and non-alcoholic steatohepatitis (NASH) are unknown.



* Corresponding author. Address: Department of Pharmacology, Toxicology and Therapeutics, University of Kansas Medical Center, MS 1018, 3901 Rainbow Blvd., Kansas City, Kansas 66160, USA. Tel: 913-588-8999. hni@kumc.edu (H.-M. Ni).

Authors' contributions

XJ. participated in performed experiments, data analysis and interpretation and preparation of manuscript; SF., FD., SC., YX., XC., XH., CM. and EMM. performed experiments, data analysis and interpretation; JT., EMM., FL., WL, LL., YZ., TL., NOD. and WXD. assisted in the design of the experiments, data interpretation and contributed to the writing of the manuscript; HMN. participated in research design, performed experiments, data analysis and interpretation, and wrote the manuscript. All authors read and approved the final manuscript.

Conflict of interest

The authors who have taken part in this study declare that they have nothing to disclose.

Please refer to the accompanying ICMJE disclosure forms for further details.

Supplementary data

Supplementary data to this article can be found online at https://doi.org/10.1016/j.jhep.2022.04.010.

**Methods:** Liver-specific and hepatocyte-specific *Vmp1* knockout mice as well as *Vmp1* knock-in mice were generated by crossing $Vmp1^{flox}$ or $Vmp1^{KI}$ mice with albumin-Cre mice or by injecting AAV8-TBG-cre, respectively. Lipid and energy metabolism in these mice were characterized by metabolomic and transcriptome analyses. Mice with hepatic overexpression of VMP1 who were fed a NASH diet were also characterized.

**Results:** Hepatocyte-specific deletion of *Vmp1* severely impaired VLDL secretion resulting in massive hepatic steatosis, hepatocyte death, inflammation and fibrosis, which are hallmarks of NASH. Mechanistically, loss of *Vmp1* led to decreased hepatic levels of phosphatidylcholine and phosphatidylethanolamine as well as to changes in phospholipid composition. Deletion of *Vmp1* in mouse liver also led to the accumulation of neutral lipids in the ER bilayer and impaired mitochondrial beta-oxidation. Overexpression of VMP1 ameliorated steatosis in diet-induced NASH by improving VLDL secretion. Importantly, we also showed that decreased liver VMP1 is associated with NAFLD/NASH in humans.

**Conclusions:** Our results provide novel insights on the role of VMP1 in regulating hepatic phospholipid synthesis and lipoprotein secretion in the pathogenesis of NAFLD/NASH.

**Lay summary:** Non-alcoholic fatty liver disease and its more severe form, non-alcoholic steatohepatitis, are associated with a build-up of fat in the liver (steatosis). However, the exact mechanisms that underly steatosis in patients are not completely understood. Herein, the authors identified that the lack of a protein called VMP1 impairs the secretion and metabolism of fats in the liver and could therefore contribute to the development and progression of non-alcoholic fatty liver disease.

## Graphical Abstract

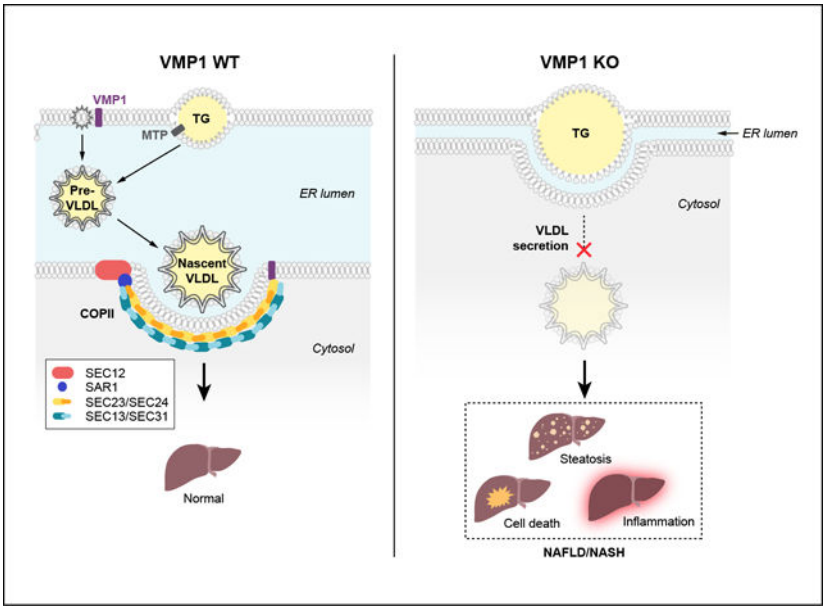


### Keywords

VLDL; endoplasmic reticulum; NAFLD; autophagy; liver injury

## Introduction

Increased free fatty acid uptake and *de novo* lipogenesis account for the majority of the hepatic fat source in non-alcoholic fatty liver disease (NAFLD).[1] Hepatic fat accumulation usually results in increased hepatic VLDL synthesis and secretion, which act as an adaptive mechanism to attenuate intrahepatic fat accumulation. Impaired hepatic VLDL secretion such as by microsomal triglyceride transfer protein (MTP) inhibition causes profound hepatic steatosis, and factors regulating hepatic VLDL synthesis and secretion are critical in modulating non-alcoholic steatohepatitis (NASH) progression and severity.[2–4]

Vacuole membrane protein 1 (VMP1) is an endoplasmic reticulum (ER) transmembrane protein which was originally identified in acute pancreatitis with vacuole formation.[5] Subsequent studies revealed that VMP1 is crucial for autophagosome and lipid droplet (LD) formation.[6,7] VMP1 is also known to regulate the secretion of soluble or specific proteins that are transported via the ER-to-Golgi trafficking pathway to maintain organelle homeostasis in *Drosophila* and *Dictyostelium*.[8,9] A recent study revealed that loss of VMP1 causes lipoprotein accumulation in the intestine, liver cells of zebrafish and early embryos of mice, as well as in human hepatoma cells, suggesting VMP1 plays a critical role in lipoprotein secretion.[10] VMP1 has phospholipid scramblase activity that regulates the cellular distribution of cholesterol and phosphatidylserine, which may be involved in LD biogenesis and SARS-CoV-2 (as well as other coronavirus) infections.[11,12]

However, the pathophysiological relevance of VMP1-regulated lipoprotein secretion in the context of NAFLD/NASH is unknown. Herein, we comprehensively characterized the function of VMP1 in regulating hepatic lipid homeostasis and VLDL secretion through physiological, biochemical, molecular and genetic rescue studies. Our findings provide novel insights and identify VMP1 as a target for NAFLD/NASH.

## Materials and methods

### Animals

*Vmp1*$^{flox}$ mice were purchased from the European Mouse Mutant Archive. *Vmp1* conditional knock-in (KI) mice were generated in collaboration with Cyagen (for details see supplementary materials). *Vmp1*$^{flox}$/*Vmp1*$^{KI}$ mice were generated by crossing *Vmp1*$^{flox}$ mice with *Vmp1*$^{KI}$ mice. To generate liver-specific *Vmp1* (L-*Vmp1*) knockout (KO) mice, *Vmp1*$^{flox}$ mice were crossed with albumin-Cre mice. To generate hepatocyte-specific *Vmp1* (H-*Vmp1*) KO or *Vmp1* restoration mice (H-*Vmp1* KO/KI), 8–10-week-old mice were injected intravenously with adeno-associated virus 8 (AAV8)-thyroxine binding globulin promoter (TBG)-null or AAV8-TBG-cre ($1\times10^{11}$ GC/mouse). All mice were fed with a chow diet unless otherwise indicated. To generate a model of diet-induced NASH, mice were fed a CDAHFD (choline-deficient, amino acid-defined high-fat diet (45% fat) containing 0.1% methionine) for 6 weeks. Mice were specific pathogen free and maintained in a barrier rodent facility under standard experimental conditions. All procedures were approved by the Institutional Animal Care and Use Committee of the University of Kansas Medical Center.

### Statistical analysis

Data were analyzed using SigmaPlot. All experimental data are expressed as mean ± SEM and subjected to unpaired Student's *t* test (2 group comparisons) or one-way ANOVA with Holm-Sidak *post hoc* test (multigroup comparisons).

Additional reagents and experimental procedures are provided in the CTAT table and supplementary materials and methods. RNAseq data are accessible from GEO (GSE186642).

## Results

### Hepatocyte-specific deletion of *Vmp1* causes accumulation of neutral lipids in mouse livers

To investigate the physiological functions of VMP1 in mice, *Vmp1*$^{flox}$ mice were injected with AAV8-TBG-null (wild-type, H-WT) or AAV8-TBG-cre (hepatocyte-specific *Vmp1* KO, H-*Vmp1* KO) for 1, 2 and 4 weeks. Compared to H-WT mice, H-*Vmp1* KO mice had enlarged and yellowish livers (Fig. 1A), with a time-dependent increase in liver weight and liver-body weight ratio, but decreased body weight at 4 weeks post AAV injection (Fig. 1A,B). Contiguous patches of micro-steatosis, hepatocyte ballooning, lobular inflammation and accumulation of hepatic lipids were revealed by H&E and Oil Red O staining in H-*Vmp1* KO mice (Fig. 1C). Levels of hepatic triglyceride (TG) and cholesterol markedly increased in H-*Vmp1* KO mice compared with H-WT mice (Fig. 1D). In contrast, steady-state serum levels of TG and cholesterol significantly decreased in H-*Vmp1* KO mice, although at 4 weeks serum levels of cholesterol in H-*Vmp1* KO mice had recovered to almost the same levels as in H-WT mice (Fig. 1E). Hepatic LDLR levels decreased in H-*Vmp1* KO mouse livers compared with WT mice (Fig. 1F), which may contribute to increased serum cholesterol at 4 weeks post AAV injection. H-*Vmp1* KO mice at 4 weeks post AAV injection had similar energy expenditure (Fig. S1A) and respiratory exchange ratio (Fig. S1B) but significantly decreased activity and lean mass compared to H-WT mice (Fig. S1C,D), suggesting sickness of the mice may contribute to decreased bodyweight.

Both male and female H-*Vmp1* KO mice exhibited similar increases in liver-body weight ratio (Fig. S2A), levels of hepatic TG and cholesterol (Fig. S2B). However, female H-*Vmp1* KO mice had lower serum levels of TG, but higher levels of cholesterol compared with male H-*Vmp1* KO mice (Fig. S2C). Similar to H-*Vmp1* KO mice, L-*Vmp1* KO mice also showed decreased body weight, increased liver-body weight ratio but similar liver weight (Fig. S3A,B), severe hepatic steatosis (Fig. S3C), increased hepatic TG and cholesterol contents (Fig. S3D) and decreased serum TG and cholesterol (Fig. S3E). Hepatocytes isolated from L-*Vmp1* KO mice or from *Vmp1*$^{flox}$ mice infected with adenovirus cre showed increased numbers of LD compared with WT hepatocytes (Fig. S3F–G). These data indicate that VMP1 plays a critical role in regulating hepatic lipid homeostasis in mice.

### Deletion of hepatocyte *Vmp1* impairs lipoprotein secretion in mice

Compared with matched WT mice, levels of serum TG and TG secretion rate significantly decreased in H-*Vmp1* KO and L-*Vmp1* KO mice following intravenous administration of

tyloxapol to block lipolysis and uptake of circulating TG-rich lipoproteins (Fig. 2A,B). Immunoblot analysis showed decreased liver and serum levels of apolipoprotein (APO)B100 in L-*Vmp1* KO mice and H-*Vmp1* KO mice at 1, 2 but not 4 weeks post AAV injection (Fig. 2C,D). Radiolabeled APOB100 and APOB48 also decreased in H-*Vmp1* KO mice with less effect on APOB48 (Fig. 2E). Interestingly, levels of serum APOB and hepatic VMP1 recovered in H-*Vmp1* KO mice at 4 weeks post AAV injection (Fig. 2D,F) but TG secretion was only partially improved (Fig. 2G). Hepatic mRNA levels of *Apob* significantly decreased in both H-*Vmp1* and L-*Vmp1* KO mice (Fig. 2H), suggesting a possible downregulation of APOB by deletion of hepatic *Vmp1*. Intriguingly, some hepatocytes still had VMP1 expression with fewer LDs, and were PCNA (proliferating cell nuclear antigen)-positive at 4 weeks post AAV injection (Fig. S4A,B), suggesting increased compensatory hepatocyte proliferation. These data suggest that the recovery of VMP1 and APOB proteins in H-*Vmp1* KO mice is likely due to compensatory proliferation from cells in which *Vmp1* was not sufficiently deleted by cre.

Levels of LC3-II increased after starvation in WT hepatocytes, which further increased in the presence of chloroquine (CQ), suggesting increased autophagic flux. The basal levels of p62 and LC3-II were much higher in *Vmp1* KO hepatocytes compared with WT hepatocytes, suggesting impaired autophagy in *Vmp1* KO hepatocytes. The levels of LC3-II were also further increased by CQ treatment in *Vmp1* KO hepatocytes, which is likely due to the incomplete deletion of VMP1 (Fig. S5A). Results of a RFP-GFP-LC3 puncta assay showed that starvation increased the number of red-only puncta in WT hepatocytes, which was markedly inhibited by CQ. *Vmp1* KO hepatocytes had increased basal levels of yellow puncta with very few red-only puncta under starvation conditions (Fig. S5B). These data indicate that *Vmp1* KO hepatocytes have impaired autophagy, which is consistent with previous findings.[10] H-*Atg5* KO mice developed hepatomegaly with elevated serum alanine aminotransferase (ALT) levels but had only slightly increased levels of hepatic TG and no change of cholesterol (Fig. S6A–D), which is consistent with our previous report that L-*Atg5* KO mice do not exhibit impaired VLDL secretion and hepatic steatosis.[13] Immunoblot analysis confirmed efficient deletion of VMP1 and ATG5 with increased SQSTM1/p62 in H-*Vmp1* and H-*Atg5* KO mouse livers. H-*Atg5* KO mice had blunted LC3-II with increased LC3-I, whereas H-*Vmp1* KO mice had increased LC3-I and LC3-II levels (Fig. S6E). These data indicate that loss of hepatic VMP1 impairs VLDL secretion and hepatic autophagy.

## Deletion of *Vmp1* in hepatocytes leads to lipid accumulation inside the ER bilayer

Lipid fractions from L-*Vmp1* KO mouse livers were enriched with calnexin (ER marker) but had less perilipin-2 (cytosolic LD marker) and almost no detectable SEC24D (coat protein complex II [COPII]) and APOB100 (lipoprotein). In contrast, lipid fractions from WT mouse livers have abundant perilipin-2, APOB100 and SEC24D but had less calnexin (Fig. 3A), suggesting that the majority of lipid fractions are within the ER in *Vmp1* KO mouse livers but are either cytosolic LDs or lipoproteins in WT mice. Oleic acid (OA) treatment markedly increased the number of perilipin-2-positive LDs in primary cultured WT hepatocytes. Increased numbers of LDs were readily observed in *Vmp1* KO hepatocytes with or without OA treatment, and most of these LDs were perilipin-2-negative with larger size compared to WT hepatocytes (Fig. 3B,C). Most LDs in *Vmp1* KO hepatocytes but not

OA-treated WT hepatocytes were positive for APOB (Fig. 3D,F) and KDEL (an ER marker, Fig. 3E,F). EM analysis of *Vmp1* KO hepatocytes revealed that "LDs" had membranes facing the cytosol (black arrows) with clear electron dense "edges" (likely representing the phospholipid monolayer) surrounding the lipid structure. The space (denoted by stars) between the ER membrane and the electron dense-edged lipid structures should be the ER lumen (Fig. 3G). Similar "LD" structures were also observed in L-*Vmp1* KO mouse livers (Fig. 3H). Taken together, these data suggest that LDs in *Vmp1* KO hepatocytes are not cytosolic LDs and are most likely within the ER bilayer, consistent with the findings reported by Morishita *et al.*[10]

## Hepatocyte deletion of *Vmp1* reduces levels of phospholipids, alters the fatty acyl chain compositions of phospholipids and decreases fatty acid beta-oxidation

Unbiased lipidomics analysis revealed that levels of hepatic phospholipids significantly decreased, whereas sphingolipids and neutral lipids significantly increased in H-*Vmp1* KO mouse livers (Fig. 4A). Levels of phosphatidylcholine (PC) and phosphatidylethanolamine (PE) significantly decreased in H-*Vmp1* KO mouse livers with striking reductions in abundance of 16:0, 18:2 and 16:0, 20:4 PC, two of the most abundant linoleoyl and arachidonoyl PC species (Fig. 4B,C). Several PE species containing linoleoyl and arachidonoyl chains were also markedly decreased in H-*Vmp1* KO mouse livers (Fig. 4C).

Transcriptome analysis revealed significant gene expression changes in H-*Vmp1* KO mouse livers, with 2,111 downregulated and 3,210 upregulated genes compared with H-WT mice (Fig. S7A). Pathway enrichment analysis showed that the top 20 downregulated pathways included metabolic pathways, complement and coagulation cascades, peroxisome and fatty acid (FA) degradation, whereas the top 20 upregulated pathways included cell adhesion molecules, hematopoietic cell lineage and cytokine-cytokine receptor interactions (Fig. S7B,C). Heatmaps of gene expression showed downregulation of several important genes involved in PC and PE synthesis, lipoprotein metabolism, FA, sterol biosynthesis and fatty acid oxidation (FAO) in H-*Vmp1* KO mouse livers (Fig. S7D–H). Consistent with RNAseq data, qPCR analysis revealed the expression of lipogenesis and cholesterol metabolism genes significantly decreased in H-*Vmp1* KO mice (Fig. S7I). The levels of lipin-1, a phosphatidate phosphatase that catalyzes diglyceride synthesis, were increased at 1 week but decreased at 2 and 4 weeks post AAV injection of H-*Vmp1* KO mice (Fig. S7J). H-*Vmp1* KO mice had increased levels of glycerol, glycerol-3-phosphate, total diglyceride and monoglyceride (Fig. S7K), consistent with accumulation of the intermediates of lipid synthesis due to a lack of new lipid synthesis.

Metabolomics analysis showed a pattern of increased FAs, such as palmitate (16:0), oleate/vaccentae (18:1), eicosapentaenoate (20:5n3), as well as increased acylcarnitine species including both monounsaturated and long-chain saturated acylcarnitine species in H-*Vmp1* KO mouse livers (Fig. 4D). The increase in both FA and acylcarnitine in liver tissues is consistent with a decrease in overall β-oxidation, which was further supported by decreased levels of beta-hydroxybutyrate in H-*Vmp1* KO mouse livers (Fig. 4E) and FA β-oxidation in *Vmp1* KO hepatocytes (Fig. 4F). The expression of FA β-oxidation genes significantly decreased in H-*Vmp1* KO mouse livers (Fig. 4G and Fig. S7H). These results indicate that

impaired FA oxidation but not *de novo* lipogenesis may contribute to hepatic steatosis in H-*Vmp1* KO mice.

### Hepatocyte deletion of *Vmp1* in mice leads to NASH

Serum levels of ALT and total bilirubin (Fig. 5A) as well as hepatic caspase-3 activity and cleaved caspase-3 increased in H-*Vmp1* KO mice (Fig. 5B). The number of TUNEL- and F4/80-positive macrophages and infiltrating myeloperoxidase-positive neutrophils as well as hepatic mRNA levels of inflammatory genes markedly increased in H-*Vmp1* KO livers (Fig. 5C,D). H-*Vmp1* KO mice showed increased liver Sirius red staining, elevated hepatic α-smooth muscle actin and hydroxyproline levels as well as expression of fibrotic genes compared with H-WT mice (Fig. 5E–G). Increased inflammation and fibrosis were also consistent with our transcriptome analysis results, as both inflammation and fibrosis were among the top upregulated genes in H-*Vmp1* KO mouse livers (Fig. S7C).

L-*Vmp1* KO mice also had increased serum ALT levels, elevated hepatic caspase-3 activity (Fig. S8A,B), increased number of liver F4/80-positive macrophages, myeloperoxidase- and LY6B-positive neutrophils (Fig. S8C), as well as increased Sirius red staining (Fig. S8D), compared with L-WT mice. The expression of *Chop* and the ratio of spliced and unspliced X box binding protein 1 (*Xbp1s*/*Xbp1u*) increased significantly in H-*Vmp1* KO mouse livers (Fig. S9A,B). While levels of BIP decreased, levels of phosphorylated eIF-2α, ATF4 and CHOP all increased in H-*Vmp1* KO mouse livers (Fig. S9C), indicating increased ER stress in H-*Vmp1* KO mice. These results indicate that hepatocyte-specific deletion of *Vmp1* leads to hepatic steatosis that progresses to NASH.

### Hepatic deletion of *Vmp1* leads to decreased COPII proteins that is rescued by hepatocyte-specific *Vmp1* knock-in

MTP is required for the lipidation of APOB during the early assembly of VLDL, and protein disulfide isomerase (PDI) increases MTP activity for hepatic VLDL assembly.[3,14] No changes in the protein levels of MTP and PDI were observed in H-*Vmp1* KO mice. With the exception of SAR1A and SAR1B, levels of SEC23A, SEC24C and SEC24D, key components of COPII, decreased in H-*Vmp1* KO mice compared to H-WT mice (Fig. 6A). Restoration of *Vmp1* in *Vmp1* KO mouse livers restored all COPII proteins (Fig. 6B,C) and impaired autophagic flux, as demonstrated by decreased hepatic SQSTM1/p62 and LC3-II levels in $Vmp1^{KI}$ mice compared with $Vmp1^{flox}$ mice (Fig. 6C). Immunoprecipitation analysis revealed that VMP1 interacted with SEC24D (Fig. 6D). Immunofluorescence staining also showed increased colocalization of SEC24D with VMP1-GFP in mouse livers (Fig. 6E). Deletion of VMP1 did not affect ERLIN1 and SURF4 but decreased TANGO1 and KLHL12, which were corrected by the restoration of VMP1 (Fig. S10A,C). These data indicate that VMP1 interacts with SEC24D and hepatic deletion of *Vmp1* decreases levels of some COPII proteins. However, serum levels of albumin and α1-antitrypsin, two secretory proteins that are mediated by COPII, were comparable between H-*Vmp1* KO and H-WT mice (Fig. S10A–B), suggesting that VMP1 may play a more important role in VLDL secretion than general secretion.

### Restoration of *Vmp1* promotes VLDL secretion and attenuates NASH in H-*Vmp1* KO mice

Decreased serum TG and cholesterol levels in H-*Vmp1* KO mice were completely recovered and serum cholesterol levels further increased when *Vmp1* was restored (Fig. 7A). Fast protein liquid chromatography analysis demonstrated substantially decreased VLDL-TG levels in H-*Vmp1* KO mice, which were not only corrected but further increased in H-*Vmp1* KO mice following restoration of *Vmp1* (Fig. 7B). H-*Vmp1* KO mice had lower levels of APOB in VLDL fractions, which was completely recovered when *Vmp1* was restored (Fig. 7B). TG secretion was higher in *Vmp1*-restored mice than in H-WT mice (Fig. 7C). Following restoration of *Vmp1*, H-*Vmp1* KO mice had normal liver color and histology (Fig. 7D) as well as decreased hepatic TG contents (Fig. 7E). Restoration of *Vmp1* in H-*Vmp1* KO mice also corrected the loss of body weight, hepatomegaly and liver injury (Fig. 7F). These results indicate that restoration of *Vmp1* ameliorates impaired VLDL secretion and improves NASH in H-*Vmp1* KO mice.

### Decreased VMP1 is associated with human NAFLD livers and overexpression of VMP1 ameliorates diet-induced NASH in mice

Immunoblot and immunohistochemical analysis revealed that VMP1 decreased in human NAFLD and NASH livers (Fig. 8A,B), and NAFLD and NASH were confirmed by histology analysis (Fig. 8B). Consistent with previous reports,[15] CDAHFD-fed mice developed typical NASH and had decreased hepatic protein and mRNA levels of VMP1 (Fig. 8C). Overexpression of VMP1 significantly alleviated CDAHFD-induced decreased hepatic PC and PE levels (Fig. 8D,E), steatosis and impaired VLDL secretion (Fig. 8F–H).

## Discussion

We showed that H-*Vmp1* KO mice had severely impaired VLDL secretion, resulting in hepatic steatosis that further progressed to NASH. Three processes that occur at the ER site are critical for VLDL secretion. These include the import of neutral lipids from the ER bilayer into the ER lumen, the assembly of pre-VLDL in the ER lumen, and the export of pre-VLDL from the ER lumen to the Golgi, where VLDL further undergoes a number of modifications before being transported to the plasma membrane for secretion. Results from our biochemical and morphological studies in VMP1 KO hepatocytes and mouse livers indicate that VMP1 is required for the release of lipoproteins from the ER membrane bilayer into the ER lumen, which is consistent with findings in the intestine and liver of VMP1-deficient zebrafish and early embryos of VMP1-deficient mice and HepG2 cells.[10] However, some neutral lipids in our morphological studies seem wrapped with entire ER membrane. These structures may represent budded ER membranes with LDs, which separated from bulk ER and thus are unable to enter the secretory pathway. Moreover, as the electron microscopy sections only reflect one single section, some parts, which are not present in these sections, may not be covered by ER bilayers. 3D-electron microscopy may be necessary to further confirm these results in the future.

It is known that MTP is required for transferring the bulk of TGs into the ER lumen for VLDL assembly. MTP activity is enhanced by PDI, which is regulated by the IRE1α-XBP1s-PDI axis.[14] No significant changes in either hepatic MTP or PDI were found in

*Vmp1* KO mice, suggesting that MTP and PDI are less likely to be involved in the retention of neutral lipids in the ER membrane bilayer of *Vmp1* KO hepatocytes. The amount of PC and PE as well as the fatty acyl chain compositions of PC and PE, especially the arachidonyl chain of PC and PE, have been shown to regulate VLDL secretion.[16,17] A recent report showed that VMP1 has scramblase activity,[11] but whether loss of VMP1 may affect the equilibration of phospholipids in the ER membrane and contribute to impaired VLDL secretion remains to be investigated. However, we found that loss of VMP1 decreased hepatic PC and PE content, and altered the acyl chain composition of phospholipids. ER-mitochondria contact sites are enriched with phospholipid synthesis enzymes including phosphatidylserine synthase and phosphatidylethanolamine *N*-methyltransferase.[18] Loss of VMP1 increases ER-mitochondria contact sites in cultured COS7 cells.[7] Therefore, it is likely that VMP1 may affect biosynthesis of phospholipids by regulating ER-mitochondrial contact independent of its scramblase activity. Decreased PC and PE contents together with altered acyl chain composition of phospholipids may thus change the biophysical tension and curvature of the ER membrane that halts the import of neutral lipids from the ER membrane bilayer to the ER lumen. Future work is needed to investigate whether and how VMP1 could regulate the biosynthesis of PC and PE.

Hepatic mRNA and protein levels of APOB decreased in H-*Vmp1* KO mice. However, this could be a secondary effect due to the lack of lipoproteins in *Vmp1* KO hepatocytes, as it is known that APOB is degraded via the ER-associated degradation pathway when lipid availability is reduced.[19] It has been reported that VMP1 directly interacted with APOB100.[10] We found that VMP1 interacted with SEC24D, which raised the possibility that binding of VMP1 with APOB and SEC24D may increase the protein stability of APOB and COPII complex proteins. Future studies are needed to dissect how VMP1 might regulate hepatic APOB and COPII proteins either at the post-translational or transcriptional level or both. Nonetheless, as the majority of lipoproteins are already entrapped inside the ER membrane bilayer in *Vmp1* KO hepatocytes, decreased hepatic APOB and COPII complex proteins may not be critical for impaired VLDL secretion in *Vmp1* KO hepatocytes. Consistent with Morishita's report,[10] albumin and A1AT secretion did not seem to be impaired in H-*Vmp1* KO mice, suggesting VMP1 may be specific for VLDL but not general secretion. Interestingly, hepatic deletion of VMP1 almost abolished APOB100 secretion with moderate reduction of APOB48. Newberry *et al.* [20] reported that liver-specific *Tm6sf2* KO mice exhibited decreased VLDL secretion without changes in APOB100 and APOB48 secretion. Deletion of *Tm6sf2* in *Apobec1* KO (APOB100-only) mice led to a smaller decrease in VLDL secretion with increased APOB100 secretion compared to *Tm6sf2* KO alone while *Apobec1* KO mice had normal VLDL secretion. Those observations, coupled with our current findings suggest that the itinerary of a VLDL particle with APOB100 is distinct from that with APOB48.

Loss of hepatic VMP1 led to increased accumulation of acylcarnitines with decreased ketone bodies and $^{14}$C-palmitate oxidation, suggesting reduced FAO in *Vmp1* KO mice. Decreased FAO was also found in *Vps15*, *Atg7* and *Atg5* KO mice.[21,22] However, decreased FAO may not be the major cause of lipid accumulation in *Vmp1* KO mouse livers, as L-*Atg5* and *Atg7* KO mice do not have obvious steatosis and L-*Atg5* KO mice have normal VLDL secretion.[13,22] Moreover, zebrafish lacking *rb1cc1*/*fip200* or *atg5* also do not affect VLDL

secretion.[10] Therefore, hepatic steatosis in *Vmp1* KO mice is likely largely due to impaired VLDL secretion and less to reduced FAO and also likely independent of decrements in autophagy.

The NASH phenotypes in H-*Vmp1* KO mice are distinct from other NASH models including L-*Lpcat3* KO, *Mea6* KO, *Sar1b* KO and *Surf4* KO mice.[16,23–25] While L-*Lpcat3* KO, *Mea6* KO, *Sar1b* KO and *Surf4* KO mice all showed defective hepatic VLDL secretion and steatosis, none of them develop NASH. Notably, liver-specific *Sar1b* and *Surf4* KO mice have near-total depletion of serum TG and cholesterol, but no obvious liver damage or inflammation. Liver-specific deletion of TMEM41B, another ER lipid scramblase and homologue of VMP1, also led to impaired VLDL secretion and NASH in mice.[26] Unlike deletion of VMP1, deletion of TMEM41B does not affect levels of hepatic PC and only slightly decreased PE but increased hepatic lipogenesis without inducing ER stress. Deletion of either VMP1 or TMEM41B is sufficient to impair VLDL secretion resulting in NASH, suggesting that TMEM41B cannot compensate for the loss of VMP1 in H-*Vmp1* KO mice and vice versa. Moreover, overexpression of VMP1 is able to correct the autophagy defect in TMEM41B-deficient cells but not vice versa,[6] further supporting distinct functions of VMP1 and TMEM41B beyond lipid scramblase.

Increased cell death, inflammation and fibrosis have been observed in liver-specific *Atg5* KO mice.[27] Loss of autophagy can impair the removal of dysfunctional mitochondria resulting in decreased FAO, which can further exacerbate steatosis in *Vmp1* KO mice. Therefore, the NASH phenotypes in *Vmp1* and *Tmem41b* KO mice are likely due to combined defects in VLDL secretion and autophagy, which is unique to VMP1 and TEM41B but not for TANGO1, TALI, Mea6 and SAR1B.

In summary, our results indicate that lack of hepatic VMP1 impairs VLDL secretion and autophagy resulting in NASH. Intronic single-nucleotide polymorphism associations (rs11650106, rs2645492 and rs1292065) in the *VMP1* gene have been identified and are associated with increased levels of circulating LDL cholesterol, total cholesterol, triglyceride or decreased level of lipoprotein-associated phospholipase A2 by human genome-wide association studies.[28–31] The decreased circulating TG and cholesterol in *Vmp1* KO mice may also provide novel insights into potential strategies for preventing cardiovascular disease and atherosclerosis by targeting VMP1.

## Supplementary Material

Refer to Web version on PubMed Central for supplementary material.

## Acknowledgements

The authors acknowledge the University of Kansas Medical Center (KUMC) Liver Cell Isolation Core at Department of Pharmacology, Toxicology and Therapeutic and Liver Center for primary hepatocyte isolation and human liver samples. The authors thank KUMC Electron Microscopy Research Lab facility for assistance with the transmission electron microscope. The authors also thank Drs. Bruno Hagenbuch, Jianming Qiu and Kang Ning for helping with the radioactive experiments.

**Financial support**

The research was supported in part by NIDDK DK129234, NIAAA AA026904 (to H-M. Ni), NIAAA AA020518, AA024733 (to W-X. Ding), DK119437, HL151328 and DDRCC P30 DK052574 (to N.O. Davidson), DK121970 (to F. Li), National Institute of General Medical Sciences of COBRE grant P30GM118247 (to H. Jaeschke) and NIGMS P20GM144269 (to J. Thyfault).

## Data availability statement

RNAseq data associated with this study has been submitted to GEO database and can be accessed with the ID: GSE186642.

## Abbreviations

| | |
|---|---|
| **AAV** | adeno-associated virus |
| **ALT** | alanine aminotransferase |
| **APO** | apolipoprotein |
| **BSA** | bovine serum albumin |
| **COPII** | coat protein complex II |
| **CQ** | chloroquine |
| **ER** | endoplasmic reticulum |
| **FA** | fatty acid |
| **FAO** | fatty acid oxidation |
| **KI** | knock-in |
| **KO** | knockout |
| **LD** | lipid droplet |
| **MTP** | microsomal triglyceride transfer protein |
| **NAFLD** | non-alcoholic fatty liver disease |
| **NASH** | non-alcoholic steatohepatitis |
| **OA** | oleic acid |
| **PC** | phosphatidylcholine |
| **PDI** | protein disulfide isomerase |
| **PE** | phosphatidylethanolamine |
| **TBG** | thyroxine binding globulin |
| **TG** | triglyceride |
| **VMP1** | vacuole membrane protein 1 |

| | |
|---|---|
| **WT** | wild-type |
| **XBP1** | X box binding protein 1 |

## References


[1]. Cohen JC, Horton JD, Hobbs HH. Human fatty liver disease: old questions and new insights. Science 2011;332:1519–1523. [PubMed: 21700865]

[2]. Alves-Bezerra M, Cohen DE. Triglyceride metabolism in the liver. Compr Physiol 2017;8:1–8. [PubMed: 29357123]

[3]. Davidson NO, Shelness GS. APOLIPOPROTEIN B: mRNA editing, lipoprotein assembly, and presecretory degradation. Annu Rev Nutr 2000;20:169–193. [PubMed: 10940331]

[4]. Samuel VT, Shulman GI. Nonalcoholic fatty liver disease as a nexus of metabolic and hepatic diseases. Cell Metab 2018;27:22–41. [PubMed: 28867301]

[5]. Dusetti NJ, Jiang Y, Vaccaro MI, Tomasini R, Azizi Samir A, Calvo EL, et al. Cloning and expression of the rat vacuole membrane protein 1 (VMP1), a new gene activated in pancreas with acute pancreatitis, which promotes vacuole formation. Biochem Biophys Res Commun 2002;290:641–649. [PubMed: 11785947]

[6]. Morita K, Hama Y, Izume T, Tamura N, Ueno T, Yamashita Y, et al. Genome-wide CRISPR screen identifies TMEM41B as a gene required for autophagosome formation. J Cell Biol 2018;217:3817–3828. [PubMed: 30093494]

[7]. Zhao YG, Chen Y, Miao G, Zhao H, Qu W, Li D, et al. The ER-localized transmembrane protein EPG-3/VMP1 regulates SERCA activity to control ER-isolation membrane contacts for autophagosome formation. Mol Cell 2017;67:974–989 e976. [PubMed: 28890335]

[8]. Bard F, Casano L, Mallabiabarrena A, Wallace E, Saito K, Kitayama H, et al. Functional genomics reveals genes involved in protein secretion and Golgi organization. Nature 2006;439:604–607. [PubMed: 16452979]

[9]. Calvo-Garrido J, Carilla-Latorre S, Lazaro-Dieguez F, Egea G, Escalante R. Vacuole membrane protein 1 is an endoplasmic reticulum protein required for organelle biogenesis, protein secretion, and development. Mol Biol Cell 2008;19:3442–3453. [PubMed: 18550798]

[10]. Morishita H, Zhao YG, Tamura N, Nishimura T, Kanda Y, Sakamaki Y, et al. A critical role of VMP1 in lipoprotein secretion. Elife 2019;8.

[11]. Li YE, Wang Y, Du X, Zhang T, Mak HY, Hancock SE, et al. TMEM41B and VMP1 are scramblases and regulate the distribution of cholesterol and phosphatidylserine. J Cell Biol 2021:220.

[12]. Schneider WM, Luna JM, Hoffmann HH, Sanchez-Rivera FJ, Leal AA, Ashbrook AW, et al. Genome-scale identification of SARS-CoV-2 and pancoronavirus host factor networks. Cell 2021;184:120–132 e114. [PubMed: 33382968]

[13]. Li Y, Chao X, Yang L, Lu Q, Li T, Ding WX, et al. Impaired fasting-induced adaptive lipid droplet biogenesis in liver-specific Atg5-deficient mouse liver is mediated by persistent nuclear factor-like 2 activation. Am J Pathol 2018;188:1833–1846. [PubMed: 29803835]

[14]. Wang S, Chen Z, Lam V, Han J, Hassler J, Finck BN, et al. IRE1alpha-XBP1s induces PDI expression to increase MTP activity for hepatic VLDL assembly and lipid homeostasis. Cell Metab 2012;16:473–486. [PubMed: 23040069]

[15]. Xiong X, Kuang H, Ansari S, Liu T, Gong J, Wang S, et al. Landscape of intercellular crosstalk in healthy and NASH liver revealed by single-cell secretome gene analysis. Mol Cell 2019;75:644–660 e645. [PubMed: 31398325]

[16]. Rong X, Wang B, Dunham MM, Hedde PN, Wong JS, Gratton E, et al. Lpcat3-dependent production of arachidonoyl phospholipids is a key determinant of triglyceride secretion. Elife 2015;4.

[17]. Hashidate-Yoshida T, Harayama T, Hishikawa D, Morimoto R, Hamano F, Tokuoka SM, et al. Fatty acid remodeling by LPCAT3 enriches arachidonate in phospholipid membranes and regulates triglyceride transport. Elife 2015;4.

[18]. Stone SJ, Vance JE. Phosphatidylserine synthase-1 and −2 are localized to mitochondria-associated membranes. J Biol Chem 2000;275:34534–34540. [PubMed: 10938271]

[19]. Ginsberg HN, Fisher EA. The ever-expanding role of degradation in the regulation of apolipoprotein B metabolism. J Lipid Res 2009;50(Suppl):S162–S166. [PubMed: 19050312]

[20]. Newberry EP, Hall Z, Xie Y, Molitor EA, Bxayguinov PO, Strout GW, et al. Liver-specific deletion of mouse Tm6sf2 promotes steatosis, fibrosis, and hepatocellular cancer. Hepatology 2021.

[21]. Iershov A, Nemazanyy I, Alkhoury C, Girard M, Barth E, Cagnard N, et al. The class 3 PI3K coordinates autophagy and mitochondrial lipid catabolism by controlling nuclear receptor PPARalpha. Nat Commun 2019;10:1566. [PubMed: 30952952]

[22]. Saito T, Kuma A, Sugiura Y, Ichimura Y, Obata M, Kitamura H, et al. Autophagy regulates lipid metabolism through selective turnover of NCoR1. Nat Commun 2019;10:1567. [PubMed: 30952864]

[23]. Wang X, Wang H, Xu B, Huang D, Nie C, Pu L, et al. Receptor-mediated ER export of lipoproteins controls lipid homeostasis in mice and humans. Cell Metab 2020.

[24]. Santos AJ, Nogueira C, Ortega-Bellido M, Malhotra V. TANGO1 and Mia2/cTAGE5 (TALI) cooperate to export bulky pre-chylomicrons/VLDLs from the endoplasmic reticulum. J Cell Biol 2016;213:343–354. [PubMed: 27138255]

[25]. Wang Y, Liu L, Zhang H, Fan J, Zhang F, Yu M, et al. Mea6 controls VLDL transport through the coordinated regulation of COPII assembly. Cell Res 2016;26:787–804. [PubMed: 27311593]

[26]. Huang D, Xu B, Liu L, Wu L, Zhu Y, Ghanbarpour A, et al. TMEM41B acts as an ER scramblase required for lipoprotein biogenesis and lipid homeostasis. Cell Metab 2021;33:1655–1670 e1658. [PubMed: 34015269]

[27]. Ni HM, Woolbright BL, Williams J, Copple B, Cui W, Luyendyk JP, et al. Nrf2 promotes the development of fibrosis and tumorigenesis in mice with defective hepatic autophagy. J Hepatol 2014;61:617–625. [PubMed: 24815875]

[28]. Chu AY, Guilianini F, Grallert H, Dupuis J, Ballantyne CM, Barratt BJ, et al. Genome-wide association study evaluating lipoprotein-associated phospholipase A2 mass and activity at baseline and after rosuvastatin therapy. Circ Cardiovasc Genet 2012;5:676–685. [PubMed: 23118302]

[29]. Hoffmann TJ, Theusch E, Haldar T, Ranatunga DK, Jorgenson E, Medina MW, et al. A large electronic-health-record-based genome-wide study of serum lipids. Nat Genet 2018;50:401–413. [PubMed: 29507422]

[30]. Ripatti P, Ramo JT, Mars NJ, Fu Y, Lin J, Soderlund S, et al. Polygenic hyperlipidemias and coronary artery disease risk. Circ Genom Precis Med 2020;13:e002725. [PubMed: 32154731]

[31]. Richardson TG, Sanderson E, Palmer TM, Ala-Korpela M, Ference BA, Davey Smith G, et al. Evaluating the relationship between circulating lipoprotein lipids and apolipoproteins with risk of coronary heart disease: a multivariable Mendelian randomisation analysis. PLoS Med 2020;17:e1003062. [PubMed: 32203549]

## Highlights

- VMP1 is critical in regulating the homeostasis of hepatic phospholipids and lipoprotein secretion.
- Decreased hepatic VMP1 is associated with human NAFLD/NASH.
- Overexpression of VMP1 improves diet-induced NAFLD.

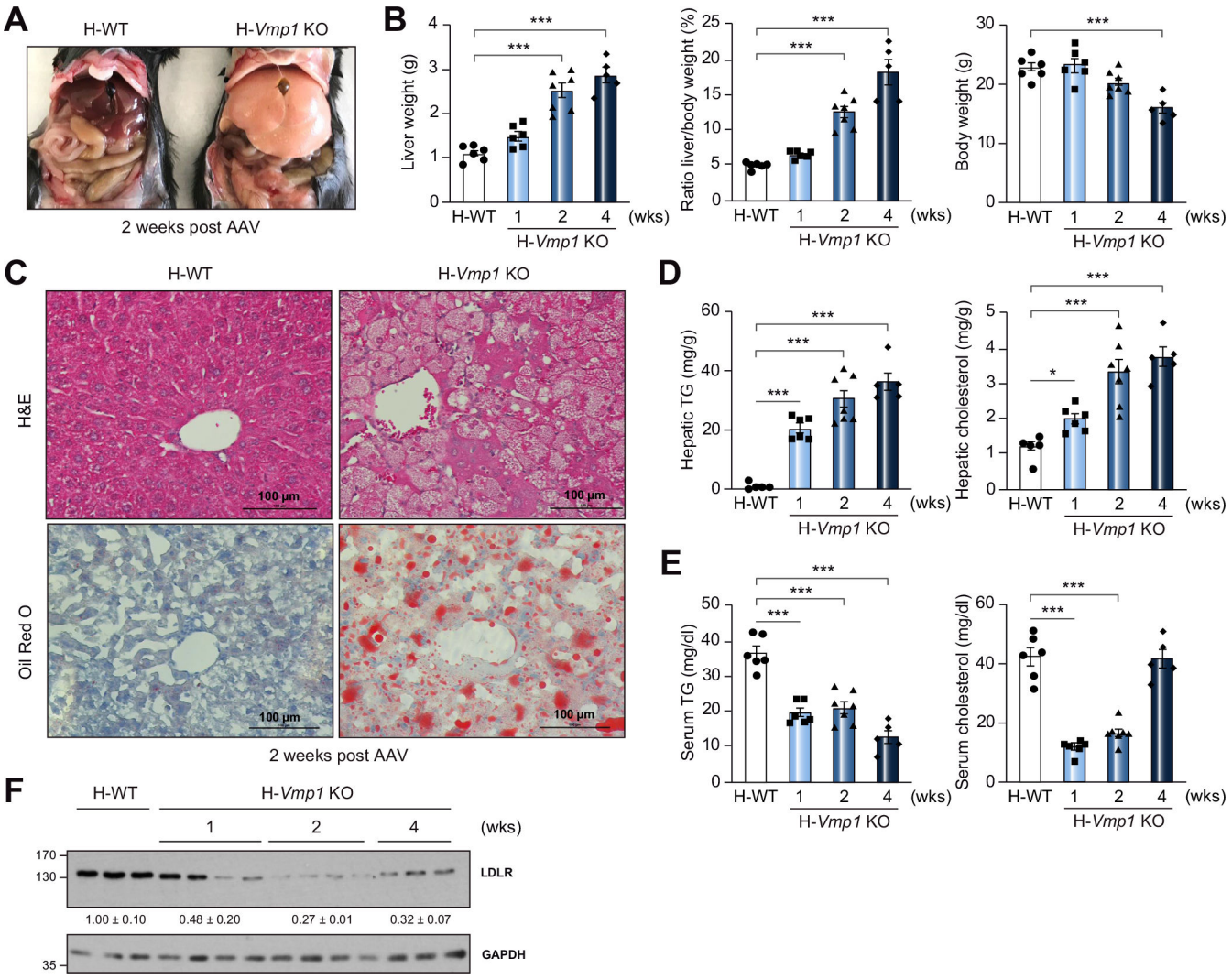


**Fig. 1. Loss of hepatic VMP1 leads to steatosis in mice.**

(A) Representative images of 8–10-week-old *Vmp1*$^{flox}$ mice at 2 weeks post AAV8-TBG-null (H-WT) or AAV8-TBG-cre (H-*Vmp1* KO) injection. (B) Mouse liver, liver/body weight ratio and body weight. (C) H&E and Oil Red O staining of liver tissues from H-WT and H-*Vmp1* KO mice. Hepatic (D) and serum (E) TG and cholesterol were quantified. (F) Total liver lysates were subjected to immunoblot analysis. Data represent mean ± SEM (n = 5–7). ** *p* <0.001 (One-way ANOVA with Holm-Sidak *post hoc* test). KO, knockout; TG, triglyceride; WT, wild-type.

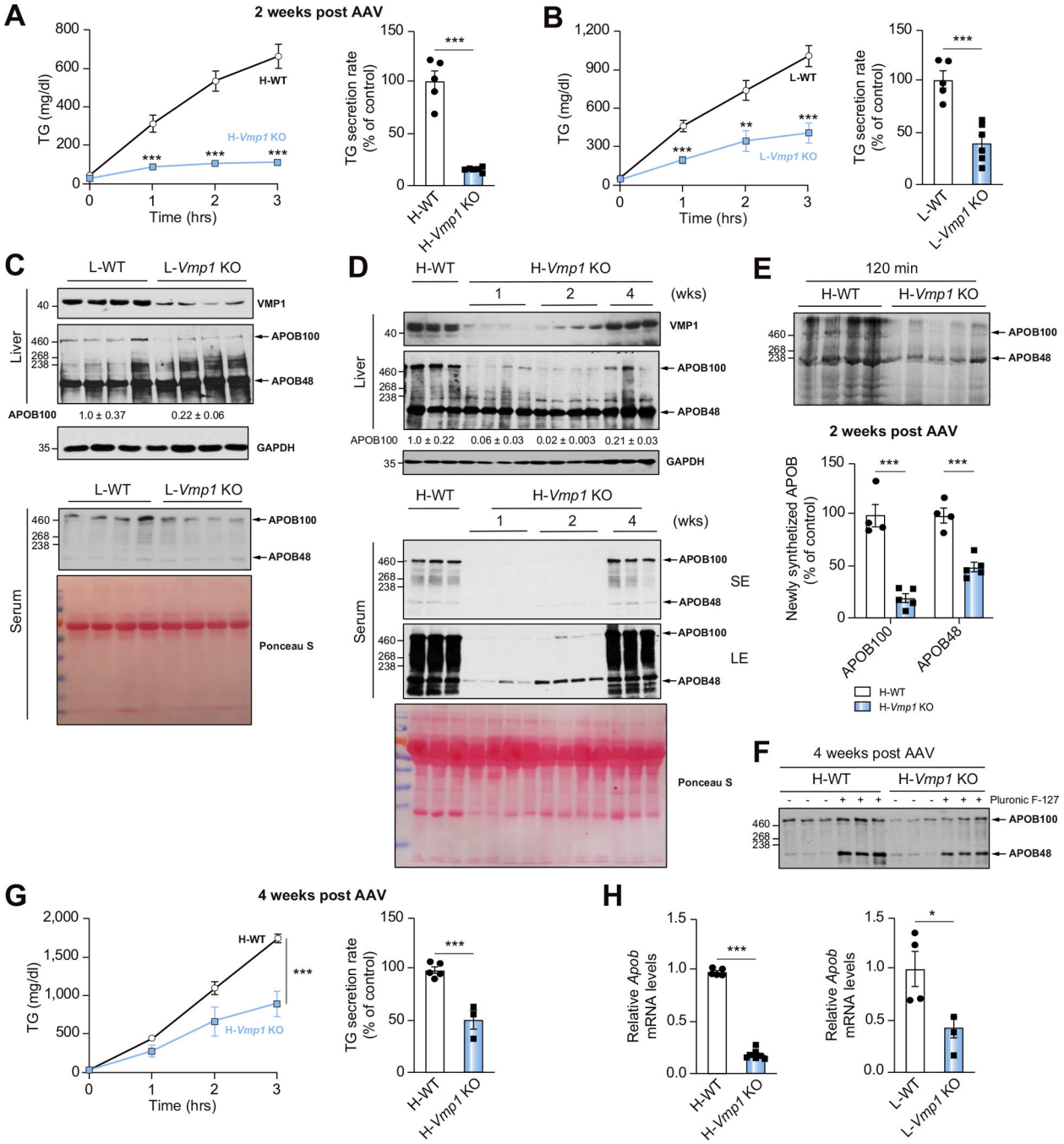


**Fig. 2. Reduced TG and lipoprotein secretion in hepatocyte-specific and liver-specific *Vmp1* KO mice.**

(A) H-WT and H-*Vmp1* KO mice or (B) one-month-old L-WT and L-*Vmp1* KO mice were injected with tyloxapol and serum TG concentrations and secretion rates were measured. Total liver lysates and serum from L-WT and L-*Vmp1* KO mice (C) or H-WT and H-*Vmp1* KO mice (D) were subjected to immunoblot analysis. (E) Mice were fasted for 4–5 hours followed by injection via tail vein with 1 mg/g Pluronic™ F-127 and 15 mCi/kg of $^{35}$S-methionine labeling mix. Newly synthesized APOB was quantified 120 minutes later in H-WT and H-*Vmp1* KO mouse sera. (F) Immunoblot analysis of serum APOB. (G)

TG concentrations and secretion rates were measured in H-WT and H-*Vmp1* KO mice at 4 weeks post AAV. (H) qPCR analysis of hepatic *Apob* mRNA. Data represent mean ± SEM (n = 4–7). *$p$ <0.05; * *$p$ <0.01; ** *$p$ <0.001 (Unpaired Student's *t* test). APO, apolipoprotein; LE, long exposure; SE, short exposure.

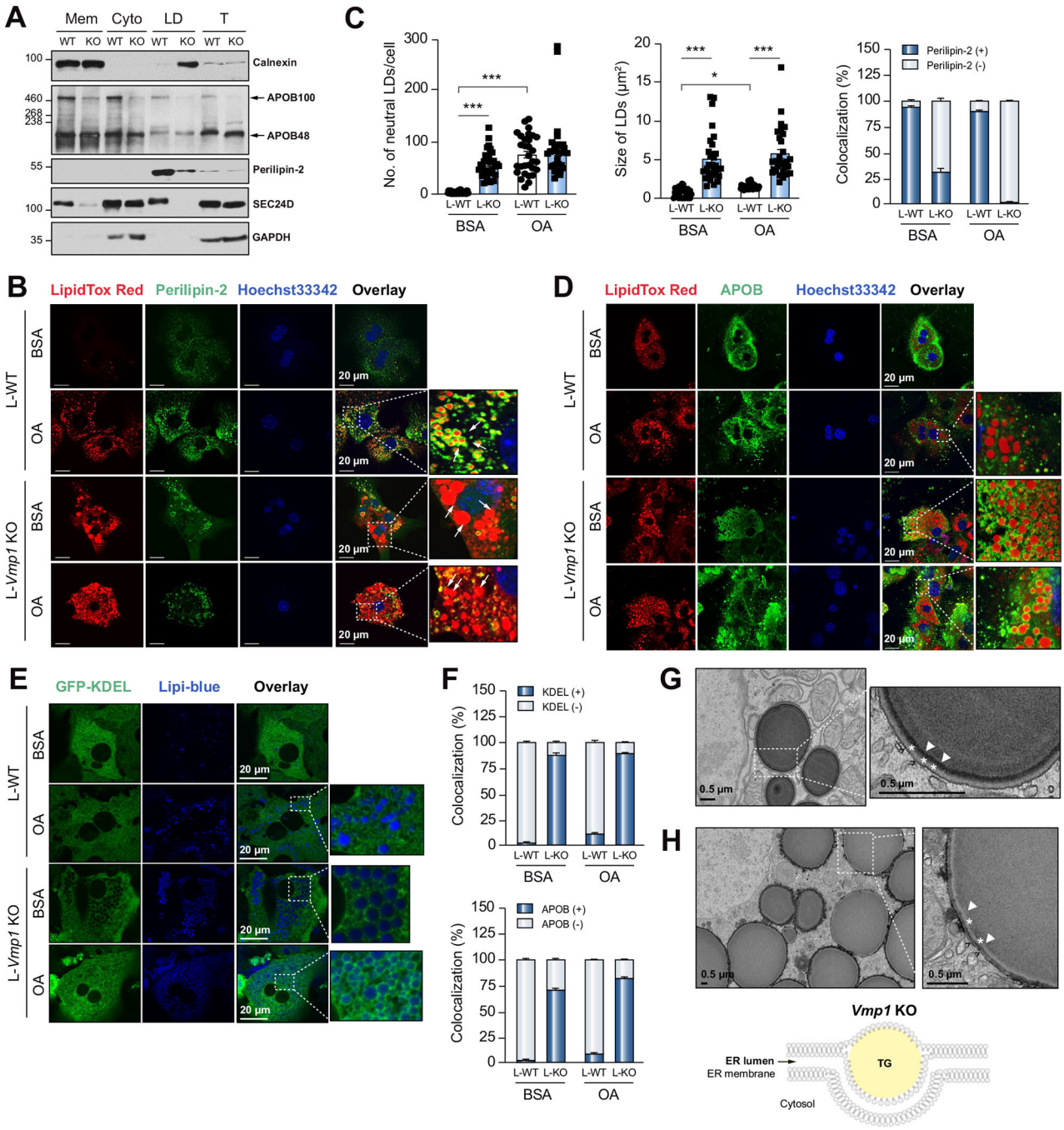


**Fig. 3. Loss of hepatic VMP1 causes accumulation of lipids in the endoplasmic reticulum bilayer.**

(A) Liver subcellular fractions were subjected to immunoblot analysis. (B) Primary hepatocytes were treated with BSA or OA (200 μM) for 6 hours and stained with perilipin-2 and LipidTOX Red followed by confocal microscopy. White arrows indicate LDs. (C) Total number, size of LDs, and colocalization of neutral lipids with perilipin-2 were quantified (≥30 cells of 3 independent experiments). (D) Primary hepatocytes were stained with APOB and LipidTOX Red followed by confocal microscopy. (E) Primary hepatocytes were infected with Ad-ssRFP-GFP-KDEL and stained with Lipi-blue followed by confocal

microscopy. (F) Colocalization of LDs with APOB and KDEL were quantitated (≥20 cells of 2 independent experiments). Representative EM images of primary hepatocyte from L-*Vmp1* KO mice (G) or H-*Vmp1* KO mouse livers at 2 weeks post AAV (H). *$p$ <0.05; ** *$p$ <0.001 (One-way ANOVA with Holm-Sidak *post hoc* test). BSA, bovine serum albumin; Cyto, cytosol; ER, endoplasmic reticulum; LD, lipid droplet; Mem, membrane; OA, oleic acid; T, total lysate.

A

Significant difference ($p \leq 0.05$) between the groups shown; metabolite ratio <1
Significant difference ($p \leq 0.05$) between the groups shown; metabolite ratio >1
Narrowly missed cutoff for significance; $0.05 < p < 0.10$; metabolite ratio <1
Narrowly missed cutoff for significance; $0.05 < p < 0.10$; metabolite ratio >1
Mean values are not significantly different for that comparison

| | Biochemical name | H-*Vmp1* KO / H-WT | |
|---|---|---|---|
| | | 1 week | 2 weeks |
| Phospholipids | Phosphatidylcholines | 0.83 | 0.73 |
| | Lysophosphatidylcholines | 0.49 | 0.35 |
| | Phosphatidylethanolamines | 0.68 | 0.41 |
| | Lysophosphatidylethanolamines | 0.62 | 0.35 |
| | Phosphatidylinositols | 1.09 | 1.44 |
| Sphingolipids | Ceramides | 1.31 | 1.64 |
| | Dihydroceramides | 1.11 | 1.38 |
| | Hexosylceramides | 1.29 | 3.23 |
| | Lactosylceramides | 0.82 | 0.78 |
| | Sphingomyelins | 0.79 | 0.63 |
| Neutral lipids | Cholesteryls esters | 7.49 | 14.47 |
| | Diacylglycerols | 2.90 | 9.15 |
| | Triacylglycerols | 9.54 | 18.54 |
| | Monoacylglycerols | 1.04 | 1.95 |

D

| Sub pathway | Biochemical name | H-*Vmp1* KO / H-WT | |
|---|---|---|---|
| | | 1 week | 2 weeks |
| Long chain saturated fatty acid | myristate (14:0) | 3.16 | 4.29 |
| | pentadecanoate (15:0) | 1.85 | 2.13 |
| | palmitate (16:0) | 2.14 | 2.32 |
| | margarate (17:0) | 3.63 | 3.65 |
| | stearate (18:0) | 1.53 | 1.74 |
| | nonadecanoate (19:0) | 2.19 | 1.85 |
| | arachidate (20:0) | 4.20 | 2.46 |
| Long chain monounsaturated fatty acid | myristoleate (14:1n5) | 1.96 | 3.96 |
| | palmitoleate (16:1n7) | 6.35 | 9.69 |
| | 10-heptadecenoate (17:1n7) | 5.39 | 7.55 |
| | oleate/vaccenate (18:1) | 3.30 | 3.71 |
| | 10-nonadecenoate (19:1n9) | 6.01 | 5.41 |
| | eicosenoate (20:1) | 8.02 | 5.57 |
| | erucate (22:1n9) | 5.64 | 2.46 |
| Long chain polyunsaturated fatty acid (n3 and n6) | tetradecadienoate (14:2)* | 0.86 | 1.06 |
| | hexadecatrienoate (16:3n3) | 1.36 | 3.46 |
| | heptadecatrienoate (17:3)* | 5.60 | 6.54 |
| | stearidonate (18:4n3) | 3.60 | 4.27 |
| | eicosapentaenoate (EPA; 20:5n3) | 2.91 | 2.42 |
| | heneicosapentaenoate (21:5n3) | 2.22 | 2.12 |
| | docosapentaenoate (n3 DPA; 22:5n3) | 2.92 | 2.65 |
| | docosahexaenoate (DHA; 22:6n3) | 1.36 | 1.38 |
| | nisinate (24:6n3) | 2.33 | 2.29 |
| | hexadecadienoate (16:2n6) | 4.32 | 6.21 |
| | linoleate (18:2n6) | 2.17 | 2.38 |
| | linoleate [alpha or gamma; (18:3n3 or 6)] | 3.51 | 4.41 |
| | dihomo-linoleate (20:2n6) | 5.47 | 5.15 |
| | dihomo-linolenate (20:3n3 or 6) | 2.53 | 2.46 |
| | arachidonate (20:4n6) | 1.32 | 0.97 |
| | adrenate (22:4n6) | 2.79 | 1.90 |
| | docosadienoate (22:2n6) | 4.71 | 3.20 |
| Fatty acid metabolism (acyl carnitine, long chain saturated) | palmitoylcarnitine (C16) | 1.04 | 10.26 |
| | margaroylcarnitine (C17)* | 0.59 | 7.40 |
| | stearoylcarnitine (C18) | 1.51 | 11.07 |
| | arachidoylcarnitine (C20)* | 1.04 | 5.72 |
| | behenoylcarnitine (C22)* | 0.72 | 1.35 |
| | lignoceroylcarnitine (C24)* | 1.04 | 1.54 |
| Fatty acid metabolism (acyl carnitine, monounsaturated) | palmitoleoylcarnitine (C16:1)* | 2.27 | 11.41 |
| | oleoylcarnitine (C18:1)* | 1.50 | 4.43 |
| | eicosenoylcarnitine (C20:1)* | 1.43 | 14.28 |
| | erucoylcarnitine (C22:1)* | 1.30 | 2.22 |
| | nervonoylcarnitine (C24:1)* | 1.14 | 1.44 |
| Fatty acid metabolism (acyl carnitine, polyunsaturated) | linoleoylcarnitine (C18:2)* | 1.25 | 2.56 |
| | dihomo-linoleoylcarnitine (C20:2)* | 1.00 | 8.60 |
| | arachidonoylcarnitine (C20:4) | 1.95 | 3.77 |
| | dihomo-linolenoylcarnitine (C20:3n3 or 6)* | 3.24 | 12.69 |
| | docosahexaenoylcarnitine (C22:6)* | 1.71 | 2.53 |

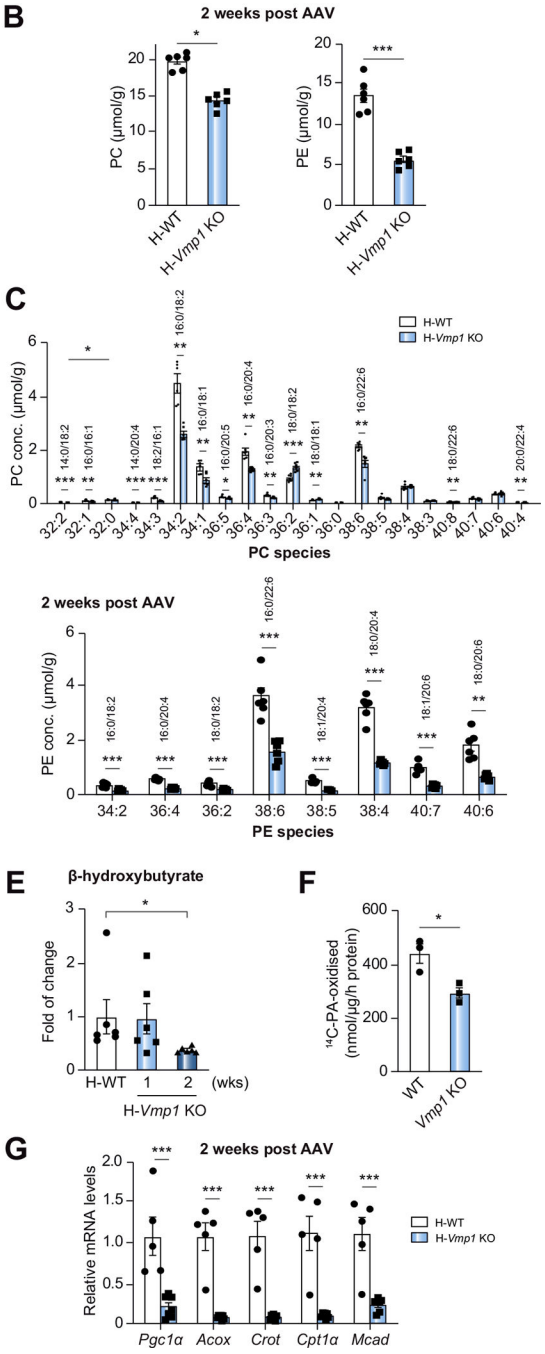


**Fig. 4. Loss of VMP1 in hepatocytes leads to reduced phospholipids and impaired fatty acid β-oxidation.**

(A) Heatmaps of phospholipids, sphingolipids and neutral lipids, (B) total PC and PE, and (C) PC and PE species by metabolomics analysis of H-WT and H-*Vmp1* KO mouse livers at 2 weeks. (D) Heatmaps of fatty acid metabolism and (E) β-hydroxybutyrate changes by metabolomics analysis. (n = 6). (F) FAO was measured in primary hepatocytes (n = 3 independent experiments). (G) qPCR analysis of hepatic FAO gene expression in mouse livers. Data represent mean ± SEM (n = 5–7). *$p$ <0.05; * *$p$ <0.01; ** *$p$ <0.001 (Unpaired

Student's *t* test for 2 group comparison or one-way ANOVA with Holm-Sidak *post hoc* test for multigroup comparison). PC, phosphatidylcholine; PE, phosphatidylethanolamine.

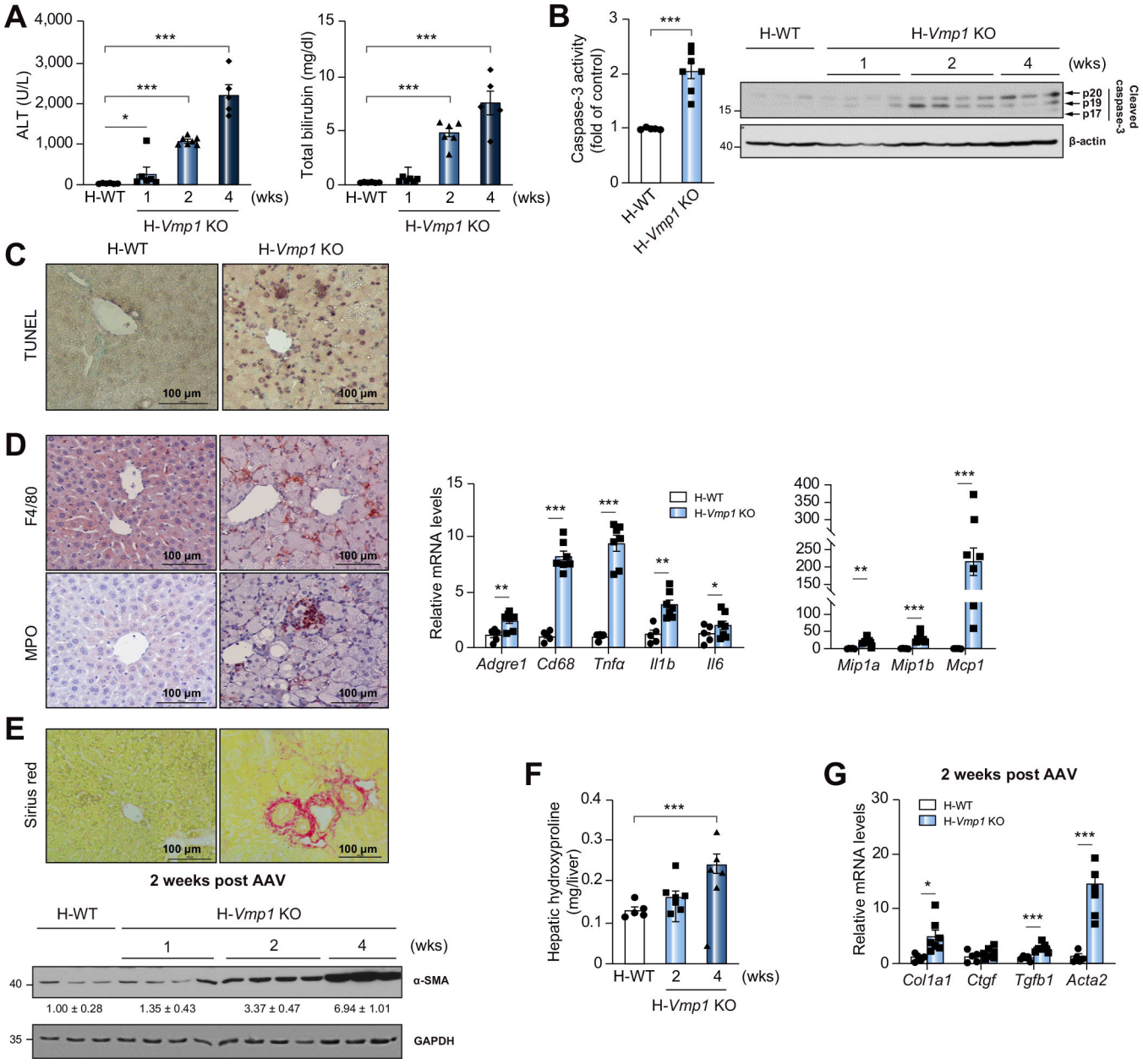


**Fig. 5. H-*Vmp1* KO mice develop NASH.**

(A) Serum ALT and bilirubin of H-WT and H-*Vmp1* KO mice were measured. (B) Caspase-3 activity and cleaved caspase-3 were analyzed using total liver lysates. (C) TUNEL staining and (D) immunohistochemistry staining for F4/80 and MPO in mouse livers as well as qPCR analysis of hepatic inflammatory genes. (E) Sirius red staining and immunoblot analysis of α-SMA in mouse livers. (F) Hepatic hydroxyproline and (G) qPCR analysis of fibrotic gene expression was quantified. Data represent mean ± SEM (n = 5–7). *$p$ <0.05; **$p$ <0.01; ***$p$ <0.001 (Unpaired Student's $t$ test for 2 group comparison or one-way ANOVA with Holm-Sidak *post hoc* test for multigroup comparison). ALT, alanine aminotransferase.

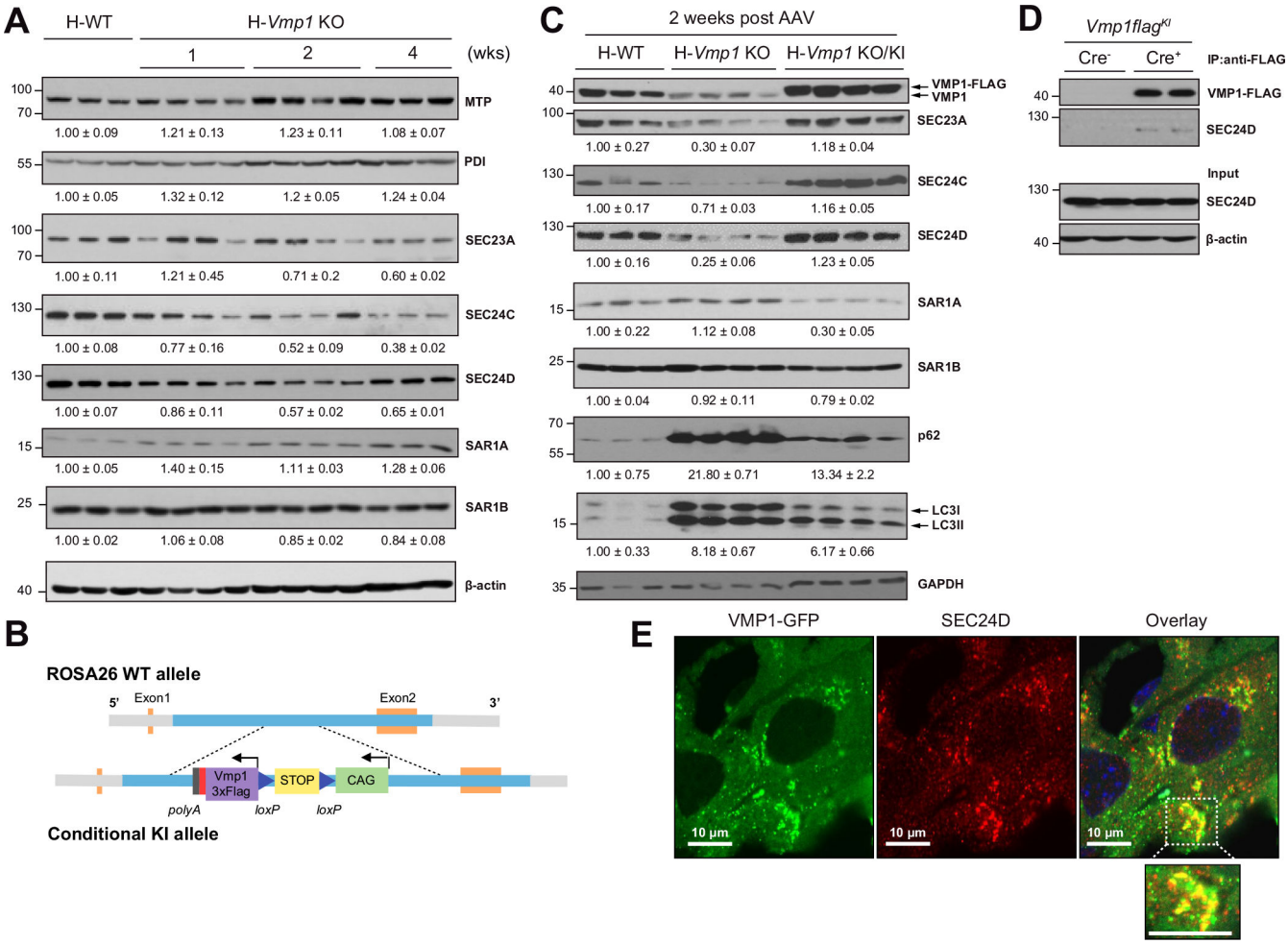


**Fig. 6. Reduced COPII in hepatic *Vmp1* KO mice.**

(A) Total liver lysates of indicated mice were subjected to immunoblot analysis. (B) Strategy for generating conditional *Vmp1*$^{KI}$ mice. (C) Total liver lysates of indicated mice were subjected to immunoblot analysis. (D) Immunoprecipitation assay for VMP1 and SEC24D in mouse livers. (E) *Vmp1*$^{flox}$ mice were injected with AAV8-TBG-cre for 1 week followed by injecting Ad-*Vmp1-Gfp* for another 2 weeks. Immunostaining for SEC24D was performed and the colocalization of VMP1-GFP and SEC24D was assessed by confocal microscopy. KI, knock-in.

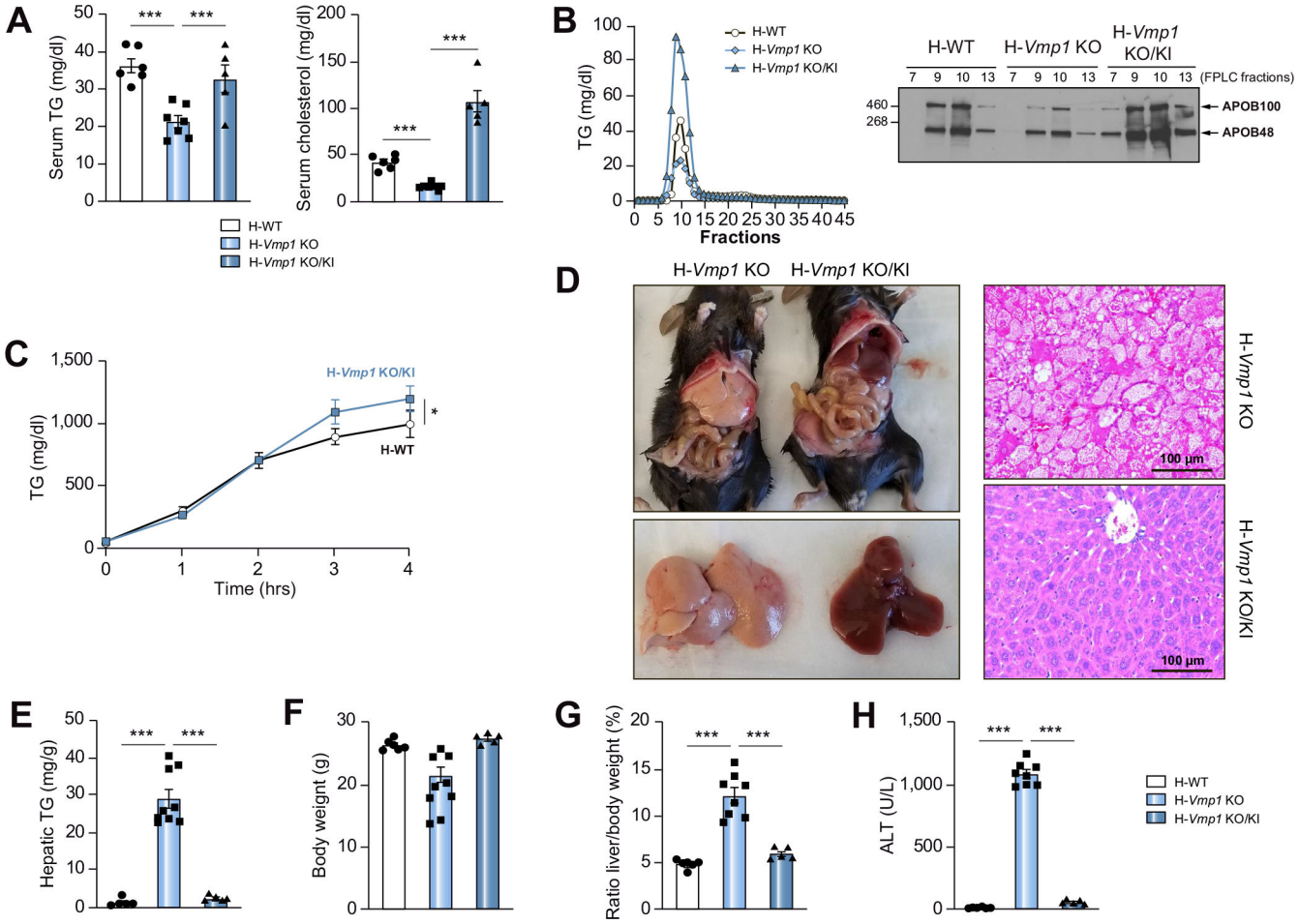


**Fig. 7. Restoration of VMP1 in *Vmp1* KO mice improves VLDL secretion and ablates hepatic steatosis and liver injury.**

(A) Serum TG and cholesterol were measured in H-WT, H-*Vmp1* KO and H-*Vmp1* KO/KI mice at 2 weeks post AAV. (B) Mice were fasted for 4 hours followed by Pluronic™ F-127 injection for another 4 hours. Pooled serum samples were subjected to FPLC analysis of lipoproteins (n = 5), and each corresponding fraction was subjected to immunoblot analysis for APOB. (C) VLDL secretion was assessed in mice after VMP1 restoration. (D) Representative images of gross livers, H&E and Oil Red O staining of mouse livers. (E-H) Hepatic TG (E), body weight (F), liver/body weight ratio (G) and ALT (H) were quantified. Data represent mean ± SEM (n = 5–7). *$p$ <0.05; ** *$p$ <0.001 (Unpaired Student's $t$ test for 2 group comparison or one-way ANOVA with Holm-Sidak *post hoc* test for multigroup comparison).

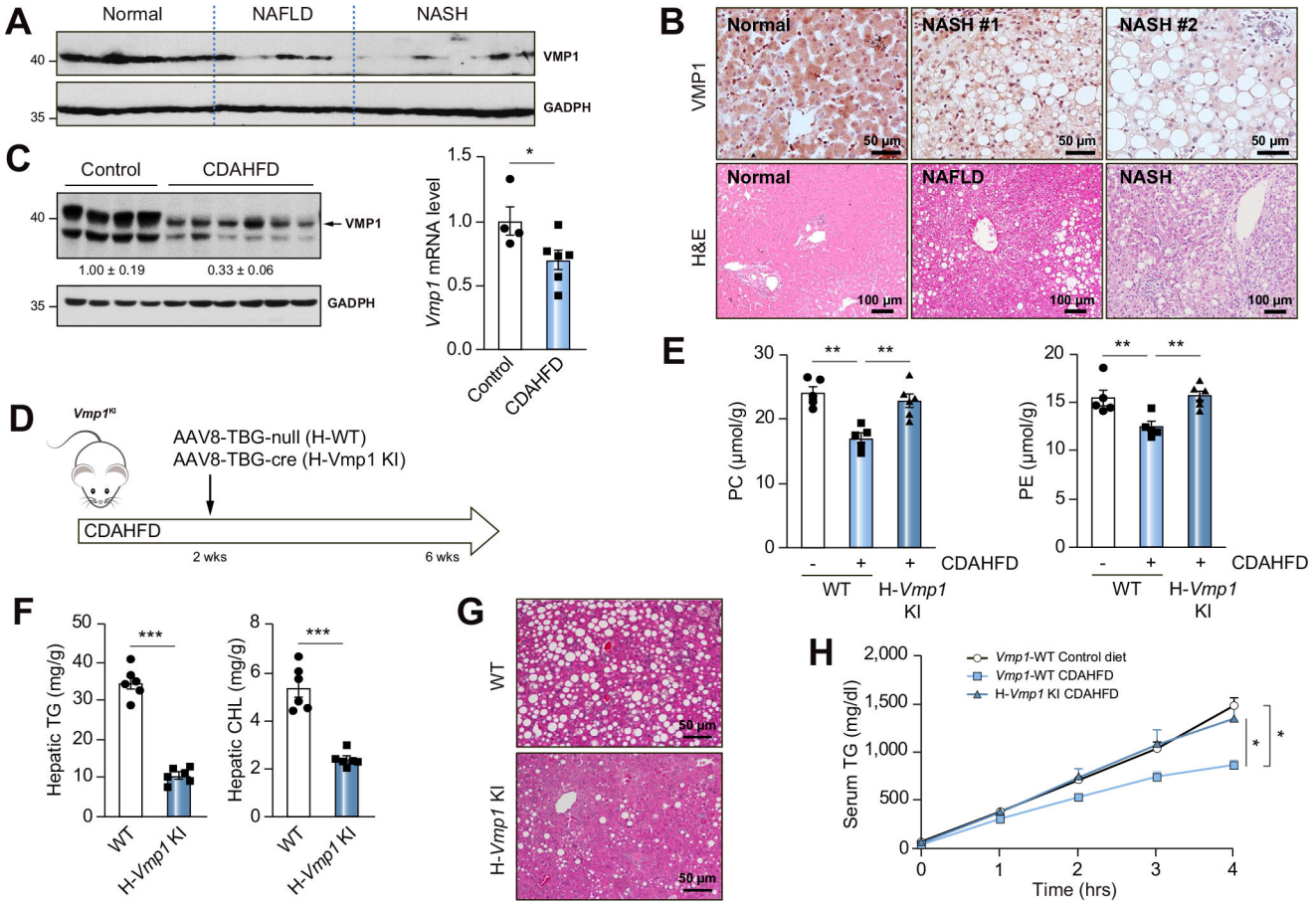


**Fig. 8. Decreased VMP1 in human NAFLD and overexpression of VMP1 alleviates diet-induced steatosis in mice.**

(A) Total lysates from human livers were subjected to immunoblot analysis. (B) Representative images of VMP1 IHC and H&E staining of normal and NAFLD/NASH patient livers. (C) H-WT mice were fed with CDAHFD for 6 weeks. Protein and mRNA levels of VMP1 in mouse livers were measured by immunoblot and qPCR analysis. (D) Scheme of CDAHFD-induced NASH in mice. (E) Hepatic concentrations of PC and PE, (F) TG and cholesterol and (G) H&E staining of liver tissues. (H) VLDL secretion was assessed in WT and VMP1 KI mice. Data represent mean ± SEM (n = 5–7). *$p$ <0.05; ** *$p$ <0.001 (Unpaired Student's $t$ test for 2 group comparison or one-way ANOVA with Holm-Sidak *post hoc* test for multigroup comparison). NAFLD, non-alcoholic fatty liver disease; NASH, non-alcoholic steatohepatitis.